



Source details

Heliyon

Open Access ⓘ

Scopus coverage years: from 2015 to 2022

Publisher: Elsevier

E-ISSN: 2405-8440

Subject area: Multidisciplinary

Source type: Journal

CiteScore 2021

4.0 ⓘ

SJR 2021

0.550 ⓘ

SNIP 2021

1.270 ⓘ

[View all documents >](#)

[Set document alert](#)

[Save to source list](#) [Source Homepage](#)

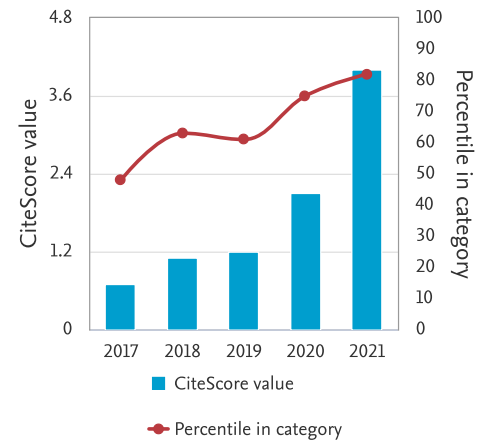
[CiteScore](#) [CiteScore rank & trend](#) [Scopus content coverage](#)

[Export content for category](#)

CiteScore rank ⓘ 2021 In category: Multidisciplinary

☆	Rank	Source title	CiteScore 2021	Percentile
☆	#22	Heliyon	4.0	82nd percentile
☆	#1	Nature	70.2	99th percentile
☆	#2	Science	57.8	98th percentile
☆	#3	Nature Communications	23.2	97th percentile
☆	#4	National Science Review	19.1	97th percentile
☆	#5	Science advances	18.5	96th percentile
☆	#6	Proceedings of the National Academy of Sciences of the United States of America	18.1	95th percentile
☆	#7	Science Bulletin	17.2	94th percentile
☆	#8	Journal of Advanced Research	17.1	93rd percentile
☆	#9	Research	10.5	92nd percentile
☆	#10	The Innovation	10.0	92nd percentile
☆	#11	Scientific Reports	6.9	91st percentile
☆	#12	Tsinghua Science and Technology	5.8	90th percentile

CiteScore trend



About Scopus

[What is Scopus](#)

[Content coverage](#)

[Scopus blog](#)

[Scopus API](#)

[Privacy matters](#)

Language

[日本語版を表示する](#)

[查看简体中文版本](#)

[查看繁體中文版本](#)

[Просмотр версии на русском языке](#)

Customer Service

[Help](#)

[Tutorials](#)

[Contact us](#)

ELSEVIER

[Terms and conditions](#) ↗ [Privacy policy](#) ↗

Copyright © Elsevier B.V. ↗. All rights reserved. Scopus® is a registered trademark of Elsevier B.V.

We use cookies to help provide and enhance our service and tailor content. By continuing, you agree to the use of cookies ↗.





Quick Turnaround Times

Publish in Orthopedic Research and Reviews & get 25% off with code DIGIT

Dove Medical Press

Heliyon 

COUNTRY

Netherlands

Universities and research
institutions in
Netherlands**SUBJECT AREA AND CATEGORY**Multidisciplinary
Multidisciplinary**PUBLISHER**

Elsevier BV

H-INDEX

46

PUBLICATION TYPE

Journals

ISSN


24058440



COVERAGE

2015-2021

INFORMATION[Homepage](#)[How to publish in this journal](#)c.schulz@cell.com**SCOPE**

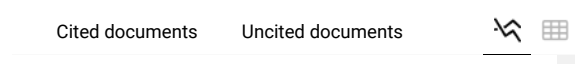
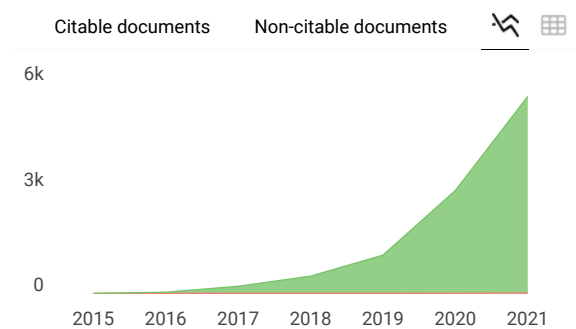
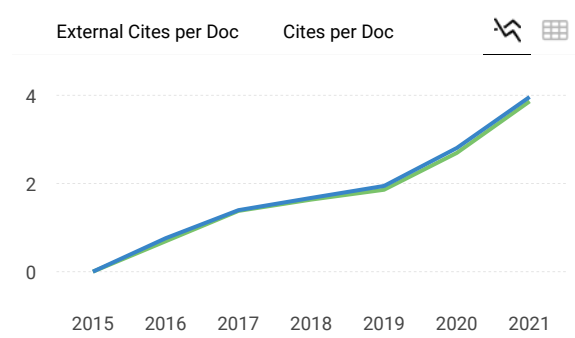
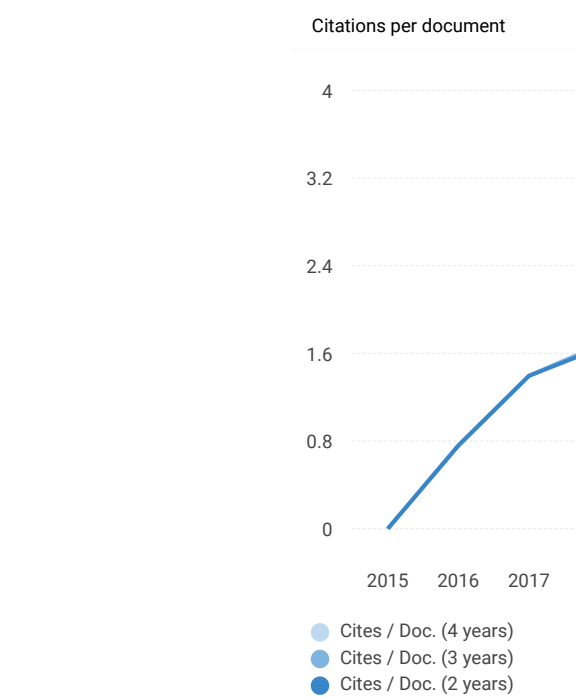
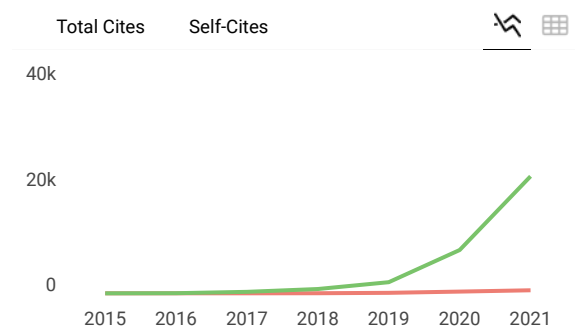
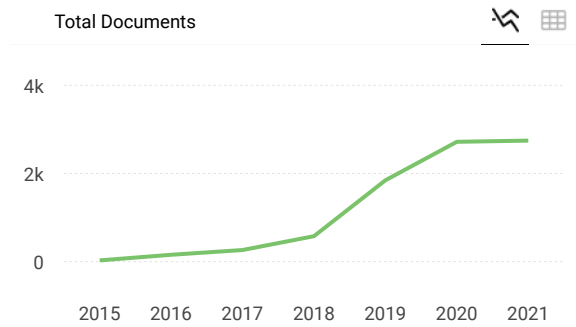
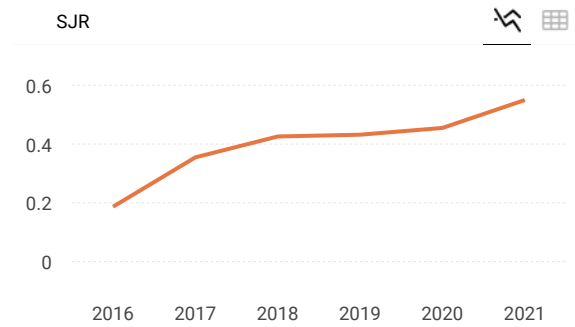
Heliyon is an all-science, open access journal that is part of the Cell Press family. Any paper reporting scientifically accurate and valuable research, which adheres to accepted ethical and scientific publishing standards, will be considered for publication. Our growing team of dedicated section editors, along with our in-house team, handle your paper and manage the publication process end-to-end, giving your research the editorial support it deserves.

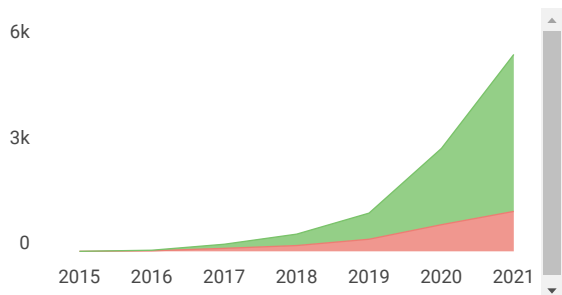
 Join the conversation about this journal

 Quartiles


FIND SIMILAR JOURNALS ?

<p>1 Journal of Advanced Research EGY</p> <p>53% similarity</p>	<p>2 Scientific African NLD</p> <p>51% similarity</p>	<p>3 Journal of Global Pharma Technology IND</p> <p>50% similarity</p>	<p>4 Current Pharmac Biotechnology NLD</p> <p>49% similarity</p>
---	---	--	--





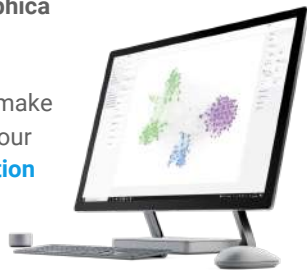
← Show this widget in your own website

Just copy the code below and paste within your html code:

``

SCImago Graphica

Explore, visually communicate and make sense of data with our [new data visualization tool](#).



Metrics based on Scopus® data as of April 2022



Mubbasher munir 3 months ago

Hi

What is the status of journal in 2022?

Is it recognized yet?

reply



Melanie Ortiz 3 months ago

SCImago Team

Dear Mubbasher,

Thank you very much for your comment.

All the metadata have been provided by Scopus /Elsevier in their last update sent to SCImago, including the Coverage's period data. The SJR for 2021 was released on 11 May 2022. We suggest you consult the Scopus database directly to see the current index status as SJR is a static image of Scopus, which is changing every day.

The Scopus' update list can also be consulted here:

<https://www.elsevier.com/solutions/scopus/how-scopus-works/content>

Best Regards, SCImago Team




Mar 01, 2021


Volume 7, Issue 3

Open Access



Current issue Online Now ●●●

- Select All
-  Export Citations
-  Email A Colleague
-  Add to Reading List

 Register for eTOC alerts

Research article

Relationship between heavy metals and alpha emission rates in breast milk and blood of women

Asmaa H. Abboud, Basim A. Almayahi

e06590

[Full-Text HTML](#) | [PDF](#)



yanga pottery and the Manyika ethnohistory: towards a decolonised
archaeology of the Nyanga agricultural complex



- Correlation of quantitative diffusion weighted MR imaging between benign, malignant chondrogenic and malignant non-chondrogenic bone tumors with histopathologic type**

Rosy Setiawati, M.S. Suarnata, Paulus Rahardjo, Del Grande Filippo, Giuseppe Guglielmi
e06402

[Full-Text HTML](#) | [PDF](#)

- The study of antiviral drugs targeting SARS-CoV-2 nucleocapsid and spike proteins through large-scale compound repurposing**

Xuqiao Hu, Zhenru Zhou, Fei Li, Yang Xiao, Zhaoyang Wang, Jinfeng Xu, Fajin Dong, Hairong Zheng, Rongmin Yu
e06387

[Full-Text HTML](#) | [PDF](#)

- Study on combustion, performance and exhaust emissions of bioethanol-gasoline blended spark ignition engine**

D.Y. Dhande, Nazaruddin Sinaga, Kiran B. Dahe
e06380

[Full-Text HTML](#) | [PDF](#)

- Anxiety among the Sudanese university students during the initial stage of COVID-19 pandemic**

Isra Mohamed Yassin Abas, Isra Isameldeen Mohmmmed Mohmmedalageel, Suad Mohamed Ali
e06300

[Full-Text HTML](#) | [PDF](#)

- A comparison of microwave and ultrasound routes to prepare nano-hydroxyapatite fertilizer improving morphological and physiological properties of maize (*Zea mays* L.)**

Homa Sajadinia, Dadkhoda Ghazanfari, Kazem Naghavii, Hormozd Naghavi, Batool Tahamipur
e06094

[Full-Text HTML](#) | [PDF](#)

- Design, synthesis and evaluation of novel enzalutamide analogues as potential anticancer agents**

Ritesh P. Bhole, Rupesh V. Chikhale, Ravindra D. Wavhale, Fatmah Ali Asmary, Tahani Mazy Almutairi, Hassna Mohammed Alhajri, Chandrakant G. Bonde



Editors and staff

Heliyon's sections are supported by our in-house editorial team, which is led by lead editor Christian Schulz. The editorial team leaders and editorial assistants handle preliminary checks and other administrative tasks before passing manuscripts on to the section editors for full review.



Christian Schulz ✉

Lead editor
Netherlands



Pinak Chincholkar ✉

Senior scientific editor
India



On Ching Lo ✉

Editorial team leader
United Kingdom



Harry McGee ✉

Editorial team leader
United Kingdom



Sujitha Shiney ✉

Editorial team leader
India



Fiona Ye ✉

Editorial team leader
China



Leema George

Associate scientific
editor
India



AlphY Sebastian P

Associate scientific
editor
India



**Kavitha
Subramanian
Vignesh**

Associate scientific
editor
India



Rachael Tucker

Associate scientific
editor
United Kingdom



Luca Cannatella

Senior editorial
section manager
United Kingdom



Echo Yin

Senior editorial
section manager
China



Vincent Lasseur ✉
France



Wesley Swords ✉
US



**Wouter
Hoogenboom** ✉
US



Yang Liu ✉
China



Yi Zheng ✉
US



Yuandong Sun ✉
China



RESEARCH JOURNALS

Cell

Cancer Cell

Cell Chemical Biology

Cell Genomics

Cell Host & Microbe

Cell Metabolism

Cell Reports

Cell Reports Medicine

Cell Reports Methods

Cell Reports Physical Science



Research article

Correlation of quantitative diffusion weighted MR imaging between benign, malignant chondrogenic and malignant non-chondrogenic bone tumors with histopathologic type

Rosy Setiawati^{a,*}, M.S. Suarnata^a, Paulus Rahardjo^a, Del Grande Filippo^b, Giuseppe Guglielmi^{c,d}^a Department of Radiology, Faculty of Medicine Airlangga University, Surabaya, Indonesia^b Department of Radiology, Ente Ospedaliero Cantonale, Bellinzona, Switzerland^c Department of Clinical and Experimental Medicine, School of Medicine, Foggia University, Foggia, Italy^d Department of Radiology, School of Medicine, Foggia University, Foggia, Italy

ARTICLE INFO

Keywords:

Apparent diffusion coefficient

Bone tumors

Diffusion weighted imaging

ABSTRACT

Objectives: This study aims to determine the diffusion on weighted imaging which may help in providing characterization of Apparent Diffusion Coefficient (ADC) values in benign, malignant chondrogenic and malignant non-chondrogenic bone tumors.**Material and methods:** A retrospective study with 84 samples was conducted from October 2017 to December 2019. The samples consisted of 44 males and 40 females; the age range of 10–73 years (mean age of 32.7 years old). A Diffusion-weighted Magnetic Resonance (MR) utilizes a single-shot echo-planar imaging sequence technique with the 3T MR Scanner. We classified the types of tumors into benign, malignant chondrogenic and malignant non-chondrogenic bone tumors. The mean of ADC values from the area with lowest ADC values was selected for statistical analysis. ADC values were compared between benign, malignant chondrogenic and malignant non-chondrogenic bone tumors. Therefore, Receiver Operating Curve (ROC) analysis was done to determine optimal cut-off values. The correlation of ADC values between benign, malignant chondrogenic and malignant non-chondrogenic bone tumor with histopathologic type was also evaluated.**Results:** The mean of ADC values from the area of benign, malignant chondrogenic and malignant non-chondrogenic bone tumor were 1.55×10^{-3} mm²/s, 1.84×10^{-3} mm²/s and 1.12×10^{-3} mm²/s respectively. As a matter of fact, there was a significant difference between benign and malignant bone tumor with cut-off value of 1.15×10^{-3} mm²/s and had a sensitivity of 82%, and a specificity of 92.3%. Moreover, a significant correlation was also found between ADC values with the histopathology type of bone tumors.**Conclusion:** The ADC values of benign and malignant (chondrogenic and non-chondrogenic groups) bone tumors are different. Thus, the measurement of ADC values improves the accuracy of the diagnosis of bone tumors.

1. Introduction

MR imaging is the method of choice to detect, characterize, and to assess extension of bone tumors (Costa et al., 2011). Conventional MR imaging sequences have limited value in differentiating benign to malignant bone tumors, especially owing to their low specificity (Subhawong et al., 2012; Costa et al., 2011; Gielen et al., 2004). Advanced MR imaging techniques such as Diffusion Weighted Images (DWI) is applied to bone and soft tissue tumors to increase the ability to discriminate between benign and malignant bone tumors (Del Grande et al., 2017; Lee

et al., 2016; Wang et al., 2014; Razek et al., 2012; Oka et al., 2011; Nagata et al., 2008).

Diffusion-weighted imaging (DWI) is a well-established non contrast MR technique based on Brownian motion of water molecules (Costa et al., 2011; Wang et al., 2014) that was originally applied to neuroimaging and is nowadays a well-established technique body MRI as well (Matsushima et al., 2007; Wang et al., 2014). DWI can be considered a proxy of malignancy through the detection of tissue cellularity (Marini et al., 2007). Apparent Diffusion Coefficient (ADC) is the quantitative value of DWI and has been shown to potentially play a role to

* Corresponding author.

E-mail address: rosy-s@fk.unair.ac.id (R. Setiawati).

differentiate benign and malignant bone and soft tissue tumor (Schnapauff et al., 2009; Koh and Collins, 2007) and predicts the aggressiveness and potential response before starting a treatment (Ahlawat et al., 2015; Bley et al., 2009) High ADC values represent low cellularity tissues whereas low ADC values represent high cellularity tissues (Schnapauff et al., 2009).

The aim of this study was to analyze correlation of quantitative DWI between benign, malignant chondrogenic and malignant non-chondrogenic bone tumors with histopathologic findings.

2. Materials and methods

2.1. Population

This retrospective study was approved by the regional ethics committee and all participants signed an informed consent.

From the October 1st 2017 to December 31th 2019, 84 consecutive patients were included (44 males and 40 females with an age range between 10 to 73 years and average age ± 32.702 years). The inclusion criteria were the followings: patients with bone tumor with complete bone tumor MRI protocol including DWI sequence. Exclusion criteria were the followings: non diagnostic DWI images and patients with previous chemotherapy or radiotherapy. All bone tumors were confirmed by pathology (50 surgical biopsies and 34 percutaneous core or fine needle biopsies).

2.2. MRI protocol

All the examinations were performed on MRI 3 T (Siemens Magnetom Skyra, Siemens AG Germany) using different RF coil depending of the location of the tumor. The field of view (FOV), slice thickness and matrix were adapted to the different body regions.

The following sequences were performed on every patient; axial, sagittal and coronal T1-weighted (repetition time (TR) 672–863/echo time (TE) 9–20 ms), coronal short time inversion recovery (STIR) (TR 4000/TE 82 ms) and axial T2-weighted fat saturated (TR 4040/TE 60 ms) sequences.

DWI with ADC maps were performed in the axial plane with b values of 50 and 800 s/mm² before intravenous contrast medium administration, using a spine echo, single shot echo planar technique. The parameters where TR (4430–6640 ms), TE (55–76 ms), FOV 200–325 mm², matrix size (voxel) of 115 × 128, thickness of 5–6 mm with an interslice gap of 1.5 mm and average of 1–2.

2.3. Image interpretation

In our study, DWI images were evaluated independently using Siemens PACS workstation by two radiologists with 10 years and 20 years experience who were impartial in regard to the clinical and other radiological information. Moreover, the corresponding of ADC map to the average diffusion images was attained. Area within the lesion showed a high signal on DWI corresponding with low signal ADC maps are characterized as diffusion-limited areas. As a matter of fact, within the most restricted area of the ADC map including the areas of enhancing tumor with the lowest ADC, the circular or elliptical region of interest (ROI) was placed. It was determined by visual inspection which was assumed to have corresponded to the largest amount of cellular tissue and attempted to include the largest area of tumor within the ROI, with a minimum area of 10 mm² and a maximum of 55 mm². The mean ADC values were obtained (Figure 1) (Figure 2). When tissue heterogeneity were found, at least three measurements were conducted by each observer in the most restricted area, then the mean ADC value of the three measurements was recorded. The position of the ROI was always examined thoroughly in regard to conventional MRI. The mean ADC values from the area with lowest ADC values were selected for statistical analysis.

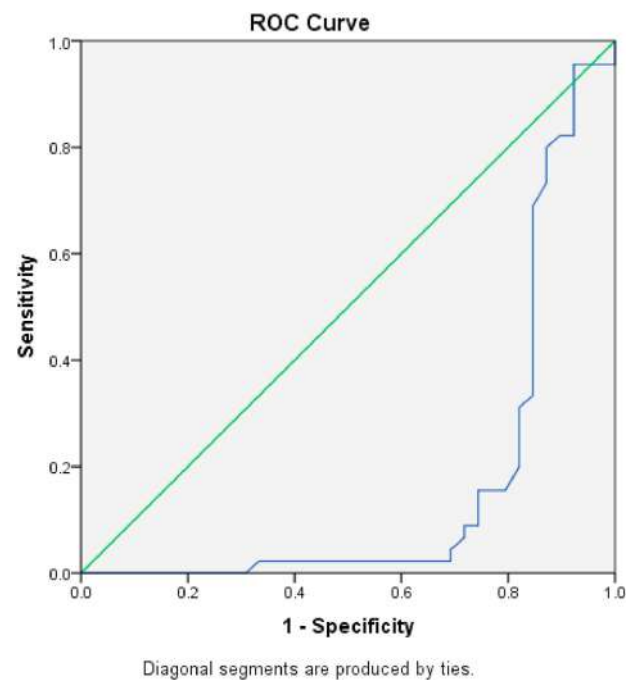


Figure 1. Receiver operating curve (ROC) curve of mean minimum apparent diffusion coefficient value for differentiation malignant and benign bone tumors. The area under the ROC curve is 0.166 (95% confidence interval 0.548–0.919).

2.4. Statistical analysis

Data analysis was performed using SPSS 23 statistics software. For statistical analysis, bone tumors were divided into benign, malignant non-chondroid, and malignant chondroid matrix, according to pathology reports. We applied receiver operating curve (ROC) analysis to determine the optimal minimum and mean cut-off of ADC values to differentiate benign, malignant chondroid tumor, and malignant non-chondroid tumor. Mann-Whitney test was used to evaluate differences in ADC values between bone tumors. Chi-square was used to assess the correlation between bone tumor DWI and ADC values with histopathological types. Inter-reader agreement of both observer was calculated with kappa test. Intraclass correlation coefficient (ICC) with $P > 0.75$ was considered as a good agreement.

3. Result

The ICCs for inter-observer agreement between the two readers was good with the kappa coefficient value of (k) = 0.003 ($p = 0.000$) at a significance level of 5%. The variability between ADC measurements was larger by using single ROI for measurement than using multiple small ROIs.

In fact, the most common age group presupposed for both benign and malignant bone tumors was 11–20 years as same as 31 cases or 36.49%. Furthermore, it was followed by 51–60 years or 18 cases with a percentage of 21.4%. Minimal number of cases were discovered in the age group of 0–10 years and >60 years with each 1.2% in one case. Thus, mean age of presentation was 32.7 years. In this study, a number of affected males were obtained as 44 or 52.3% and total number of affected females were 40 or 47.6% with the ratio 1.1:1 of M:F.

From 84 bone tumors, 41 tumors were located in the femur, 17 in the tibia, 8 in the humerus, 6 in the radius, 4 in the sacrum, 3 in the iliac wing, 2 in the acetabulum, 2 in the pedis and manus, as well as 1 in the ulna (Table 1).

Minimum ADC values, mean ADC values and p-values for benign bone tumor, malignant non-chondroid tumor, malignant chondroid tumor,

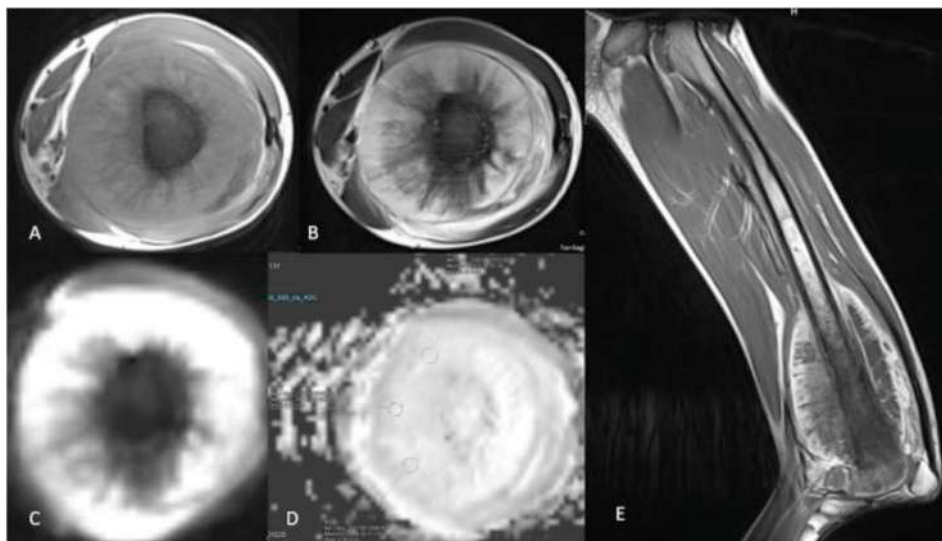


Figure 2. A 14-year-old male patient with chondroblastic type of osteosarcoma distal left femur. On MRI examination showed solid mass which appears isointense on axial T1 FSE (A), slight hyperintense on axial T2 FSE (B) and coronal T1 TSE fatsat with contrast showed contrast enhancement (E). Restricted diffusion area on DWI and slight hypointense on ADC maps (C, D) with mean ADC value of $2.27 \times 10^{-3} \text{ mm}^2/\text{s}$.

Table 1. The location of bone tumor in the study subjects.

Location	Frequency	Percentage (%)
Femur	41	48.8
Tibia	17	20.2
Humerus	8	9.5
Radius	6	7.1
Sacrum	4	4.8
Iliac wing	3	3.6
Acetabulum	2	2.4
Foot	1	1.2
Hand	1	1.2
Ulna	1	1.2
Total	84	100

and respectively are shown in the Table 2. ADC value ranged from $0.82 \times 10^{-3} \text{ mm}^2/\text{s}$ to $2.88 \times 10^{-3} \text{ mm}^2/\text{s}$ for benign tumor, from $0.78 \times 10^{-3} \text{ mm}^2/\text{s}$ to $1.67 \times 10^{-3} \text{ mm}^2/\text{s}$ for malignant non-chondroid tumor, and from $1.22 \times 10^{-3} \text{ mm}^2/\text{s}$ to $2.38 \times 10^{-3} \text{ mm}^2/\text{s}$ for malignant chondroid tumor. Mean ADC values $1.55 \times 10^{-3} \text{ mm}^2/\text{s}$ for benign tumor, $1.12 \times 10^{-3} \text{ mm}^2/\text{s}$ for malignant non-chondroid tumor, and $1.84 \times 10^{-3} \text{ mm}^2/\text{s}$ for malignant chondroid tumor (Table 3).

Table 2. The Distribution of Mean ADC Values and Standart Deviation of Bone Tumors based on the Histopathology Type.

Group of Bone Tumor	Histopatology type	ADC values		
		Frequency	Mean	Percentage (%)
Benign tumor	Osteomyelitis	6	1.5767	7.1
	Giant Cell Tumor	18	1.5139	21.4
	Aneurysmal bone cyst	3	1.6767	3.6
Malignant Chondrogenic Tumor	Chondroblastic type Osteosarcoma	8	1.7763	9.5
	Chondrosarcoma	4	1.96	4.8
Malignant Non-Chondrogenic Tumor	Osteosarcoma	27	1.1278	32.1
	Metastatic bone disease	10	1.044	11.9
	Malignant Giant Cell Tumor	3	1.165	3.6
	Plasmacytoma	4	1.2933	4.8
	Non hodkin lymphoma	1	0.78	1.2
	Total		84	

According to the ROC analysis for differentiation between malignant and benign bone tumor, the cut-off of ADC values of $1.15 \times 10^{-3} \text{ mm}^2/\text{s}$ had a sensitivity of 82%, specificity of 92.3%, and AUC (area under curve) of 0.166 (Figure 1). Cut-off difference of the ADC value between benign and malignant bone tumor is significant ($p\text{-value} = 0.000$ ($p < \alpha$)). There is a significant relationship between ADC values with the histopathology type ($p = 0.000$) (Tables 3 and 4).

4. Discussion

Our study indicates that mean ADC value supports the discrimination between benign, malignant chondrogenic tumor, and malignant non-chondrogenic bone tumors. Malignant chondrogenic bone tumors showed significantly higher mean ADC values compared to malignant non-chondroid tumor and such chondrogenic tumors should considered separately in the assessment with ADC values.

DWI is a non-contrast advanced MR technique increasingly used in body imaging (Dietrich et al., 2010). ADC represent the quantitative value of DWI and helps to differentiate high cellular from low cellular tumors (Türkbeý et al., 2012). Several studies which have utilized the qualitative DWI MRI techniques and quantitative ADC. Bone tumors with unrestricted diffusion showed high ADC values representing the presence of hypocellular and damaged cell membrane integrity which allows greater water diffusion whereas bone tumors with restricted diffusion

Table 3. The correlation between ADC values with the degree of histopathological examination between benign, malignant chondrogenic tumor and malignant non-chondrogenic tumor.

Bone tumor	Frequency	ADC values			
		Minimum ($\times 10^{-3}$ mm ² /s)	Maximum (10^{-3} mm ² /s)	Mean ($\times 10^{-3}$ mm ² /s)	SD
Benign tumor	45	0.82	2.88	1.5459	0.572
Malignant Chondrogenic tumor	12	1.22	2.38	1.8375	0.381
Malignant Non-chondrogenic tumor	27	0.78	1.67	1.1158	0.151
p values	84				0,000

Table 4. Comparison of ADC values of benign and malignant lesions of present study with other studies.

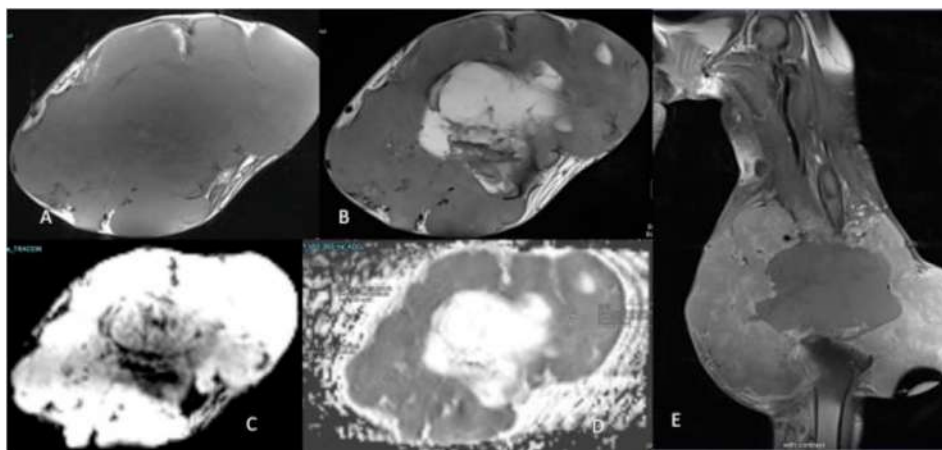
Studies	The mean ADC values of malignant lesions ($\times 10^{-3}$ mm ² /s)	The mean ADC values of benign lesions ($\times 10^{-3}$ mm ² /s)	The cut-off ADC values ($\times 10^{-3}$ mm ² /s)	The cut-off sensitivity of ADC (%)	The cut-off specificity of ADC (%)
Present study	1,48 ± 0,45	1,55 ± 0.41	1.15	82	92.3
Rao et al. (2019)	1.092 ± 0.497	1.62 ± 0.596	1.31	73.3	77.1
Pekcevik et al. (2013)	1.02 ± 1.0	1.99 ± 0.57	1.37	77.8	82.4
Wang et al. (2014)	0.87 ± 0.20	1.17 ± 0.36	1.10	89.7	84.5

showed low ADC values, representing high cellularity and intact cell membrane integrity with limited diffusion of water molecules (Bley et al., 2009). As such low ADC values are presumed to correlated with malignancy, in other hand high ADC values are presumed to correlated with benign bone tumors (Ahlawat and Fayad, 2018; Surov et al., 2015). However, ADC values can vary considerably among different studies depends on tissue type (Padhani et al., 2009), measurement techniques (minimum vs mean ADC values) (Ahlawat and Fayad, 2018) and MRI characteristics (Sasaki et al., 2008). For instance, cystic degeneration, chondroid matrix, and myxoid matrix can results in false negative of high ADC values whereas tumor with high fibrovascular tissue can results in false positive of low ADC values (Rosari et al., 2020.; Ahlawat and Fayad, 2018; Pekcevik et al., 2013; Yakushiji et al., 2009; Hayashida et al., 2006). DWI MRI is also used for monitoring therapeutic responses and a high ADC values after therapy shows a good therapeutic response. This response was likely related to necrosis or cellular lysis because of radiotherapy as well as chemotherapy, which leads to increases tissue water diffusivity, resulting in restricted diffusion area in the tumor, thus lowering signal intensity on high b value images with corresponding increases in ADC values. Because cell death in response to treatment precedes changes in lesion size, changes in DW-MRI may act as an

effective, early biomarker of response to therapy (Gaeta et al., 2014; Thoeny and Ross, 2010).

Our results showed malignant chondroid tumors had the highest ADC values among malignant tumors that 9.5% of the patients with histologic proven chondroblastic osteosarcoma had minimum ADC value higher than 1.18×10^{-3} mm²/s and mean ADC value higher than 1.77×10^{-3} mm²/s. 4.8 % of the patients with chondrosarcoma have minimum ADC values higher than 1.43×10^{-3} mm²/s and mean ADC value higher than $1,96 \times 10^{-3}$ mm²/s. 31% of the patients with histologic proven as non chondroblastic osteosarcoma had minimum ADC values lower than 0.78×10^{-3} mm²/s and mean ADC values higher than $1,13 \times 10^{-3}$ mm²/s (Table 2) (Figure 2). The studies of Rao et al.; Shivani et al.; Pekcevik et al.; Hayashida et al.; Yakushiji et al. consistently obtained similar results (Rao et al., 2019; Ahlawat and Fayad, 2018; Geneidi et al., 2016; Pekcevik et al., 2013; Neubauer et al., 2012; Ginat et al., 2012; Yakushiji et al., 2009; Hayashida et al., 2006).

We speculated that the water molecules are relatively free to spread inside the chondroid matrix compared to osteoid matrix, resulting in higher ADC values. This statement was supported by study conducted by Ahlawat S and Fayad LM (Ahlawat and Fayad, 2018), noted that high water content of hyaline cartilage in chondrogenic lesions leads to overall high ADC values. This was similar to myxoid tumor that shows

**Figure 3.** A 31-year-old woman with GCT in the distal left femur. MRI examination showed isointense solid mass with a central necrotic on axial T1 FSE and T2 FRFSE (B), and coronal T1 TSE fatsat with contrast showed contrast enhancement in the solid component part(E). Solid tumor component showed peripheral restrictive diffusion area on DWI and hypointense on ADC maps (C, D) with mean ADC value of 1.10×10^{-3} mm²/s.

higher ADC values compared to non-myxoid tumors regardless malignant or benign etiology. By increasing osteoid matrix at expanses of chondroid matrix, there will be an increasing DWI restriction and decreasing ADC values (Matsushima et al., 2007). Similar results were reported by Nagata et al. (2008), that recommended cartilaginous tumors with a chondroid matrix to be classified separately where both benign and malignant tumors with a chondroid matrix component have high ADC values and further studies need to be conducted to distinguish ADC values from benign and malignant tumors with the chondroid matrix. Jifei Wang et al. (2017), stated in their study that extracellular matrix cartilage with high water components and hyper-permeability may also produces higher ADC values.

For malignant non chondrogenic tumor, the minimum ADC values of malignant bone tumors was $0.78 \times 10^{-3} \text{ mm}^2/\text{s}$ that belonged to bone metastases and Non-Hodgkin lymphoma. These result was consistent with study by Pekcevik et al. (2013), which obtained all bone metastases ($n = 5$) below the cut-off value of ADC with a minimum ADC value of $0.67 \times 10^{-3} \text{ mm}^2/\text{s}$ and a maximum of $1.02 \times 10^{-3} \text{ mm}^2/\text{s}$. Furthermore, study conducted by Cao et al. (Cao et al., 2017), metastasis ($n = 7$) with a minimum ADC value of $0.79 \times 10^{-3} \text{ mm}^2/\text{s}$ and a maximum ADC value of $1.10 \times 10^{-3} \text{ mm}^2/\text{s}$. In this study, Plasmacytoma ($n = 4$) and Non-Hodgkin lymphoma ($n = 1$) had ADC values below the cut-off (mean ADC value $1.29 \times 10^{-3} \text{ mm}^2/\text{s}$ and $0.78 \times 10^{-3} \text{ mm}^2/\text{s}$) with DWI's interpretation of all restricted diffusions.

In our study, giant cell tumors have heterogeneous ADC values, that divided into three malignant giant cell tumors that had lower mean ADC values of $1.16 \times 10^{-3} \text{ mm}^2/\text{s}$ and 18 giant cell tumors with mean ADC value of $1.51 \times 10^{-3} \text{ mm}^2/\text{s}$, respectively (Table 2) (Figure 3). This result is similar to Pekcevik et al. and Nagata et al. (Pekcevik et al., 2013; Nagata et al., 2008). Nagata et al. reported in their study that the lower ADC value found in malignant giant cell tumors might be related to their histology in the form of adequate vascularized network of round, oval, or spindle-shaped stromal cells and multinucleated giant cells which probably decrease the extracellular space and result in decreased ADC values (Nagata et al., 2008).

Our study has limitation that the distribution of samples of benign bone tumor were predominantly giant cell tumors, which tend to have lower ADC values, also influenced the result of cut-off value in differentiating malignant from benign bone tumor. This study needs to be continued with more control group in each subtype of tumor. From malignant bone tumor group, the evaluation of ADC value study in osteosarcoma subtypes is also needed to provide more specific result.

5. Conclusion

In differentiating malignant from benign bone tumors and tumor like lesions, DWI is considerably helpful. Despite some overlapping occurred, ADC values of benign and malignant bone tumors seem to be different, so that the measurement of ADC values enriches the accuracy of bone tumors diagnosis. Our study demonstrated a significant correlation between ADC values of benign, malignant chondrogenic and malignant non chondrogenic bone tumors with histopatologic type.

Declarations

Author contribution statement

Rosy Setiawati and Giuseppe Guglielmi: Conceived and designed the experiments; Analyzed and interpreted the data; Contributed reagents, materials, analysis tools or data; Wrote the paper.

Suarnata: Performed the experiments; Contributed reagents, materials, analysis tools or data; Wrote the paper.

Paulus Rahardjo: Performed the experiments; Analyzed and interpreted the data; Contributed reagents, materials, analysis tools or data;

Filippo Del Grande: Conceived and designed the experiments; Analyzed and interpreted the data; Wrote the paper.

Funding statement

This research did not receive any specific grant from funding agencies in the public, commercial, or not-for-profit sectors.

Data availability statement

Data will be made available on request.

Declaration of interests statement

The authors declare no conflict of interest.

Additional information

No additional information is available for this paper.

References

- Ahlawat, S., Fayad, L.M., 2018 Aug 1. MR imaging of chondrogenic tumors: update on select imaging challenges. *Curr. Radiol. Rep.* 6 (8), 1–13.
- Ahlawat, S., Khandheria, P., Subhawong, T.K., Fayad, L.M., 2015. Differentiation of benign and malignant skeletal lesions with quantitative diffusion weighted MRI at 3 T. *Eur. J. Radiol.* 84 (6), 1091–1097 [Internet].
- Bley, T.A., Wieben, O., Uhl, M., 2009. Diffusion-weighted MR imaging in musculoskeletal radiology: applications in trauma, tumors, and inflammation. *Magn. Reson. Imaging. Clin. N. Am.* 17 (2), 263–275.
- Cao, J., Xiao, L., He, B., Zhang, G., Dong, J., Wu, Y., et al., 2017. Diagnostic value of combined diffusion-weighted imaging with dynamic contrast enhancement MRI in differentiating malignant from benign bone lesions. *Clin. Radiol.* 72 (9), 793.e1–793.e9.
- Costa, F.M., Canella, C., Gasparotto, E., 2011. Advanced magnetic resonance imaging techniques in the evaluation of musculoskeletal tumors. *Radiol. Clin. N. Am.* 49 (6), 1325–1358 [Internet].
- Del Grande, F., Ahlawat, S., Subhangwong, T., Fayad, L.M., 2017. Characterization of indeterminate soft tissue masses referred for biopsy: what is the added value of contrast imaging at 3.0 tesla? *J. Magn. Reson. Imag.* 45 (2), 390–400.
- Dietrich, O., Biffar, A., Baur-melnyk, A., Reiser, M.F., 2010. Technical aspects of MR diffusion imaging of the body. *Eur. J. Radiol.* 76 (3), 314–322 [Internet].
- Gaeta, M., Benedetto, C., Minutoli, F., D'Angelo, M., 2014. Use of diffusion-weighted, intravoxel incoherent motion, and dynamic contrast-enhanced MR imaging in the assessment of response to radiotherapy of lytic bone metastases from breast cancer. *Acad. Radiol.* 21 (10), 1286–1293.
- Geneidi, E.A.S., Ali, H.I., Dola, E.F., 2016. Role of DWI in characterization of bone tumors. *Egypt J. Radiol. Nucl. Med.* 47 (3), 919–927 [Internet].
- Gielen, J.L.M.A., De Schepper, A.M., Vanhoenacker, F., Parizel, P.M., Wang, X.L., Sciort, R., et al., 2004. Accuracy of MRI in characterization of soft tissue tumors and tumor-like lesions. A prospective study in 548 patients. *Eur. Radiol.* 14 (12), 2320–2330.
- Ginat, D.T., Mangla, R., Yeane, G., Johnson, M., Ekholm, S., 2012. Diffusion-weighted imaging for differentiating benign from malignant skull lesions and correlation with cell density. *Am. J. Roentgenol.* 198 (6), 597–601.
- Hayashida, Y., Hirai, T., Yakushiji, T., Katahira, K., Shimomura, O., Imuta, M., et al., 2006. Evaluation of diffusion-weighted imaging for the differential diagnosis of poorly contrast-enhanced and T2-prolonged bone masses: initial experience. *J. Magn. Reson. Imag.* 23 (3), 377–382.
- Koh, D.M., Collins, D.J., 2007. Diffusion-weighted MRI in the body: applications and challenges in oncology. *Am. J. Roentgenol.* 188 (6), 1622–1635.
- Lee, S.Y., Jee, W.H., Jung, J.Y., Park, M.Y., Kim, S.K., Jung, C.K., et al., 2016. Differentiation of malignant from benign soft tissue tumours: use of additive qualitative and quantitative diffusion-weighted MR imaging to standard MR imaging at 3.0 T. *Eur. Radiol.* 26 (3), 743–754.
- Marini, C., Iacconi, C., Giannelli, M., Cilotti, A., Moretti, M., Bartolozzi, C., 2007. Quantitative diffusion-weighted MR imaging in the differential diagnosis of breast lesion. *Eur. Radiol.* 17 (10), 2646–2655.
- Matsushima, N., Maeda, M., Takamura, M., Takeda, K., 2007. Apparent diffusion coefficients of benign and malignant salivary gland tumors. Comparison to histopathological findings. *J. Neuroimaging.* 34 (3), 183–189.
- Nagata, S., Nishimura, H., Uchida, M., Sakoda, J., Tonan, T., Hiraoka, K., et al., 2008. Diffusion-weighted imaging of soft tissue tumors: usefulness of the apparent diffusion coefficient for differential diagnosis. *Radiat. Med. - Med. Imaging Radiat. Oncol.* 26 (5), 287–295.
- Neubauer, H., Evangelista, L., Hassold, N., Winkler, B., Schlegel, P.G., Köstler, H., et al., 2012. Diffusion-weighted MRI for detection and differentiation of musculoskeletal tumorous and tumor-like lesions in pediatric patients. *World J. Pediatr.* 8 (4), 342–349.

- Oka, K., Yakushiji, T., Sato, H., Fujimoto, T., Hirai, T., Yamashita, Y., et al., 2011. Usefulness of diffusion-weighted imaging for differentiating between desmoid tumors and malignant soft tissue tumors. *J. Magn. Reson. Imag.* 33 (1), 189–193.
- Padhani, A.R., Liu, G., Mu-Koh, D., Chenevert, T.L., Thoeny, H.C., Takahara, T., et al., 2009. Diffusion-weighted magnetic resonance imaging as a cancer biomarker: consensus and recommendations. *Neoplasia* 11 (2), 102–125 [Internet].
- Pekcevik, Y., Kahya, M.O., Kaya, A., 2013. Diffusion - weighted magnetic resonance imaging in the diagnosis of bone Tumors : preliminary results. *J. Clin. Imaging Sci.* 3 (4), 1–6.
- Rao, A., Sharma, C., Paramalli, R., 2019. Role of diffusion-weighted mri in differentiating benign from malignant bone tumors. *BJR Open* 120180048, 1–9.
- Razek, A., Nada, N., Ghaniem, M., Elkhamary, S., 2012. Assessment of soft tissue tumours of the extremities with diffusion echoplanar MR imaging. *Radiol. Med.* 117 (1), 96–101.
- Rosari, C.K., Setiawati, R., Suharmanto, D., et al., 2020. B value variation using adc mapping technique with diffusion weighted imaging sequence to distinguish musculoskeletal tumor malignancy. *Mal. J. Med. Health Sci.* 16 (16), 62–66.
- Sasaki, M., Yamada, K., Watanabe, Y., Matsui, M., Ida, M., Fujiwara, S., et al., 2008. Variability in absolute apparent diffusion coefficient values across different platforms may be substantial: a multivendor, multi-institutional comparison study. *Radiology* 249 (2), 624–630.
- Schnapauff, D., Zeile, M., Niederhagen, M Ben, Fleige, B., Tunn, P.U., Hamm, B., et al., 2009. Diffusion-weighted echo-planar magnetic resonance imaging for the assessment of tumor cellularity in patients with soft-tissue sarcomas. *J. Magn. Reson. Imag.* 29 (6), 1355–1359.
- Subhawong, T.K., Wang, X., Durand, D.J., Jacobs, M.A., Carrino, J.A., Machado, A.J., et al., 2012. Proton MR spectroscopy in metabolic assessment of musculoskeletal lesions. *Am. J. Roentgenol.* 198 (1), 162–172.
- Surov, A., Nagata, S., Razek, A.A.A., Tirumani, S.H., Wienke, A., Kahn, T., 2015 Jul 28. Comparison of ADC values in different malignancies of the skeletal musculature: a multicentric analysis. *Skeletal Radiol.* 44 (7), 995–1000.
- Thoeny, H.C., Ross, B.D., 2010. Predicting and monitoring cancer treatment response with diffusion-weighted MRI. *J. Magn. Reson. Imag.* 32, 2–16.
- Türkbey, B., Aras, Ö., Karabulut, N., Turgut, A.T., Akp, E., Alibek, S., et al., 2012. Diffusion-weighted MRI for detecting and monitoring cancer: a review of current applications in body imaging. *Diagnostic Interv. Radiol.* 18 (1), 46–59.
- Wang, T., Wu, X., Cui, Y., Chu, C., Ren, G., Li, W., 2014. Role of apparent diffusion coefficients with diffusion-weighted magnetic resonance imaging in differentiating between benign and malignant bone tumors. *World J. Surg. Oncol.* 12 (1), 1–6.
- Wang, J., Sun, M., Liu, D., Hu, X., Pui, M.H., Meng, Q., et al., 2017. Corellation between apparent diffusion coefficient and histopathology subtypes of osteosarcoma after neoadjuvant chemotherapy. *Acta Radiol.* 58 (8), 971–976.
- Yakushiji, T., Oka, K., Sato, H., Yorimitsu, S., Fujimoto, T., Yamashita, Y., et al., 2009. Characterization of chondroblastic osteosarcoma: gadolinium-enhanced versus diffusion-weighted MR imaging. *J. Magn. Reson. Imag.* 29, 895–900.